

## CHAPTER ONE HUNDRED TWENTY

### Field Investigations of Suspended Sediment Transport in the Nearshore Zone

R.W. Sternberg\*, N.C. Shi<sup>†</sup>, and John P. Downing<sup>††</sup>

#### ABSTRACT

The suspended sediment distribution and longshore sediment transport characteristics at Leadbetter Beach, Santa Barbara, California were investigated using a series of miniature optical backscatter sensors which can measure particle concentrations as high as 180 gm/l and have 10 Hz frequency response. Vertical arrays of sensors were maintained at up to four positions across the surf zone during 7-25 February 1980 and were operated concurrently with pressure sensors and current meters. Data were collected on a daily basis over 2-4 hour periods.

The data were analyzed to reveal concentration profiles of suspended sediment, the average suspended sediment loads, and the longshore particle flux in relation to varying wave conditions. Results show that sediment transport occurs as individual suspension events related to incident wave motions and infragravity motion oscillations within the surf zone; suspended sediment concentration decreases approximately logarithmically away from the seabed; the maximum values of longshore transport rates occur in the mid-surf zone; and the measured suspended sediment longshore transport rate is equal to the total longshore transport rate as predicted by existing transport equations.

#### INTRODUCTION

As part of the Nearshore Sediment Transport Study (NSTS) carried out at Leadbetter Beach, Santa Barbara, California, in January-February 1980 (7), an extensive series of suspended sediment measurements were made concurrently with observations of wave motions (currents and water level fluctuations), sediment characteristics, and beach profiles. The total NSTS experiment was broad in scope, integrating a wide variety of research objectives (20,21,22). This project emphasized suspended sediment transport, with major objectives of characterizing the temporal and spatial suspended sediment distribution across the surf zone and investigating the relationship between surf zone physical processes and the littoral transport of suspended sediment. In addition, the longshore transport models of (16,17) were evaluated with respect to the longshore component of suspended sediment flux measured during a range of incident wave conditions.

\* School of Oceanography, University of Washington, Seattle, WA 98195  
† Virginia Institute of Marine Science, Gloucester Point, VA 23062  
†† Northern Technical Services, 117 Lake Street South, Kirkland, WA 98033

## STUDY AREA

Leadbetter Beach is a relatively straight sandy beach located directly updrift from the breakwater-harbor area of Santa Barbara, California (Fig. 1). It was selected as a study site because the approaching wave direction is reasonably constant due to the narrow window between the offshore Channel Islands and because the high angle of wave incidence provides a nearly unidirectional longshore current from west to east, i.e., from the study site towards the Santa Barbara breakwater which represents a total sediment trap. Semidiurnal tides have a mean range of 110 cm and a mean tide level of 85.3 cm (MLLW). The beach has a steep slope and the surf zone is narrow. The textural properties of the beach sand indicate that it is fine to medium (mean = 0.236 mm) with a sorting coefficient of 0.40.

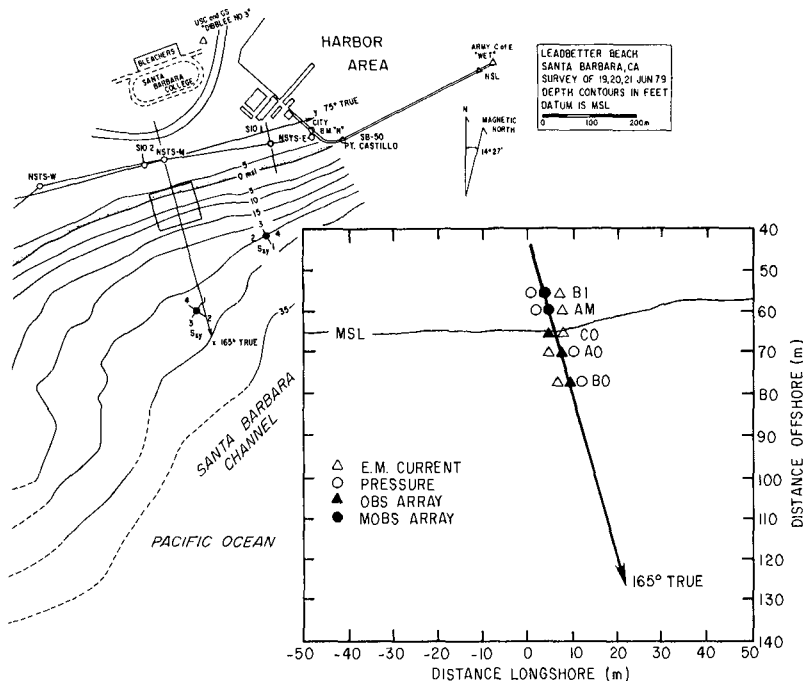


Fig. 1. Study site, including main cross-shore transect and expanded view showing instrument locations.

## TECHNIQUES

## Suspended sediment sensors

Suspended sediment concentration was measured with an optical backscatter sensor (OBS) developed at the University of Washington (4). An OBS sensor consists of a stainless steel housing 19 mm in diameter by 11 mm in length (Fig. 2). It houses an infrared emitting diode (IRED) with peak radiant intensity at 950 nm, a silicon photovoltaic cell with peak spectral response at 900 nm, and an appropriate filter to limit transmittance from incident light. The optical components are encapsulated in the sensor head with clear epoxy resin. When operating, a scattering volume of 1.3 cc is irradiated through a 5.6 mm aperture at the geometric center of the photo-detector by a IR-beam with a half-cone angle of 14°. Backscattered radiation (110-165°) is converted to photocurrent by the detector oriented in a plane normal to the emitter beam axis and located close to it.

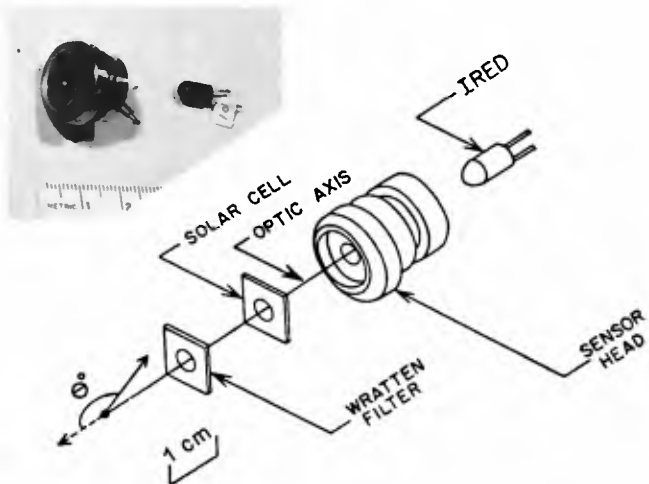


Fig. 2. OBS sensor and cut-away view.

A representative calibration curve for an OBS sensor using a beach sand with median diameter of 0.165 mm is shown in Figure 3. The response of the instrument is linear in the concentration range of 0.1 to 100 ppt by weight. The response of the instrument is minimal to air bubbles injected into the calibration tank (indicated in Fig. 3 by arrows). Each optical sensor was individually calibrated with Leadbetter Beach sediment before and after the Santa Barbara experiment. The instrument response was linear in the concentration range from 0.1 to 150 ppt and 0.1 ppt is the threshold of detection.

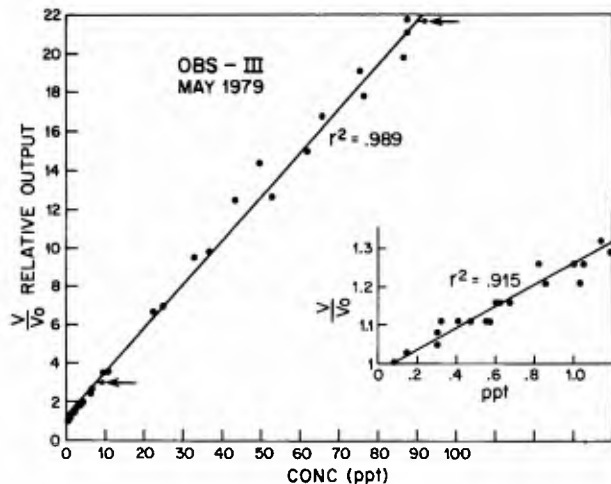


Fig. 3. Calibration curve and expanded scale for values  $<1.2$  ppt.

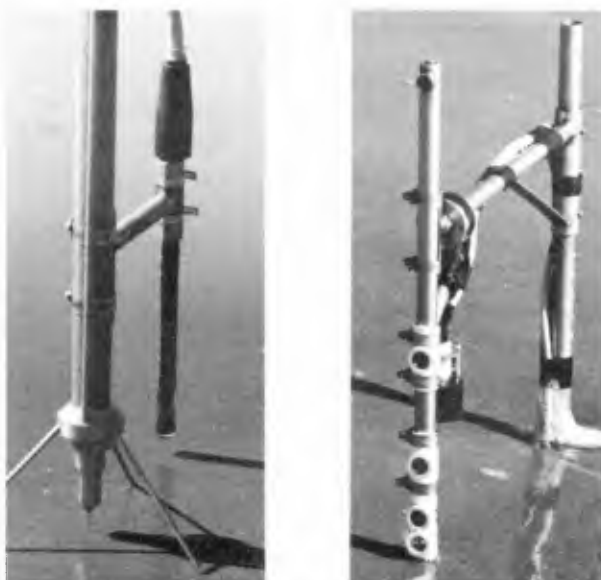


Fig. 4. MOBS (left) and OBS sensor arrays.

#### Sensor arrays

To meet the program objectives vertical arrays of OBS sensors were placed on a transect across the surf zone; vertical arrays were constructed in two sizes. An OBS array consists of five sensors mounted in a steel tube with a logarithmic spacing between sensors (Fig. 4). The total length of the array is 51 cm and the spacings between sensors is 3, 6, 12, and 30 cm. This configuration was used in the outer surf zone where water depths were >0.5 m. Plastic "shields" were fitted on the lower sensors to minimize damage from moving cobbles in the surf zone resulting from storm conditions.

A miniaturized version of the OBS array was used in the inner surf zone where water depths were generally <0.5 m. The miniature array (MOBS) consists of five OBS sensors mounted on a structural rod and encapsulated in plastic. The length of the MOBS array is 16 cm and the spacings between sensors is 3, 3, 5, and 5 cm (Fig. 4).

Up to five suspended sediment sensor arrays (OBS and MOBS) were deployed in proximity to current meters and pressure transducers placed along a primary cross-shore range line (Fig. 1). The OBS sensor arrays were cantilevered into the flow from pipes jetted into the bottom. Sensor electronics were buried in the seabed beneath each OBS sensor array and connected to the shore laboratory with a multiconductor cable. The MOBS sensor arrays were suspended from a tripod structure jetted into the upper beach face. A current meter and pressure gauge or wave staff also were mounted on each tripod. Sensor electronics were strapped on the tripod well above the sea surface and the multiconductor cable connecting the sensor electronics to the shore was buried.

All arrays were mounted vertically with the lowest sensor 3.5 cm off the seabed and the highest sensor located at 64.5 cm and 19.5 cm above the seabed for OBS and MOBS arrays, respectively. The elevation of each array was monitored before and after each data series.

OBS arrays (AO, BO, and CO) were located 6 m west of the main range line and on the same isobath as an EM current meter ( $z = 45$  cm) and a pressure sensor ( $z = 20$  cm); MOBS arrays (AMO, BMO) were located within 50 cm of an EM current meter positioned at  $z = 4$  cm (Fig. 1). All sensor output signals were transmitted continuously to the shore station and subsequently scanned and recorded in the NTS data system.

#### Data collection

The basic strategy of the sampling program was to maintain a cross-shore transect of OBS and MOBS arrays over as wide a range of wave conditions as possible. Data were collected on a daily basis between 7 and 24 February 1980. Each data series consisted of a time series of approximately 2-4 hours duration with one or more of the sensor arrays operating. Figure 5 shows the data series collected by individual sensor arrays relative to significant wave height ( $H_s$ ), which varied from about 0.3 to 1.8 m over the duration of the experiment.

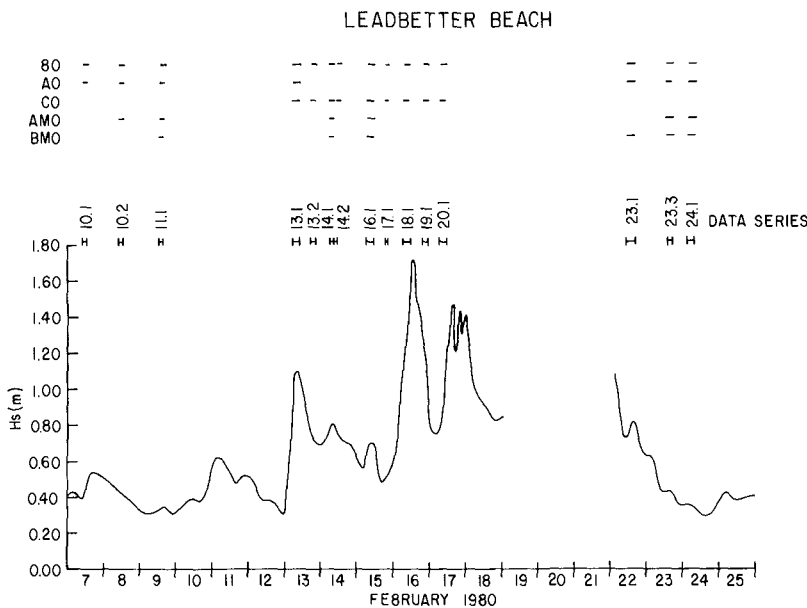


Fig. 5. Data series collected by individual sensor arrays (shown above) relative to significant wave height over the duration of the experiment.

#### ANALYSIS

##### Data set

During the experiment, 15 suspended sediment data series were collected (Fig. 5). Each consisted of continuous sampling of all operational sensor arrays, along with measurements of velocity, water level, and beach profiles (made by other NSTS investigators). For a variety of reasons it was not possible to analyze all of the data collected. Several data series were collected during periods of very low tides when sensors were not continually submerged. Also, some suspension events of nearshore sand were obscured in data collected during a severe storm because the quantity of very fine sediment in the surf zone due to storm drain flooding in Santa Barbara increased the background signal levels.

After inspecting all of the data records a data quality index was used to choose the data series that were analyzed. The primary considerations were that the data series spanned a range of wave conditions, had low background signals from washload, provided reasonable coverage

across the surf zone, and required a minimum amount of editing. Six data series (13.1, 13.2, 14.1, 14.2, 23.3, 24.1, Fig. 5) were chosen for analysis. Within these six data series, thirty segments representing different tide levels were chosen arbitrarily for averaged data analyses (34-min averages). For a tabulation of this data set see (24).

#### Suspended sediment

Three categories, high frequency data analysis, averaged data analysis, and sediment transport calculations and predictions, were employed. Initially, the raw data from all sensor outputs were block averaged to a 2 Hz sampling rate and converted to scientific units. An example of a 6 1/2-min data series is shown in Figure 6. Data included

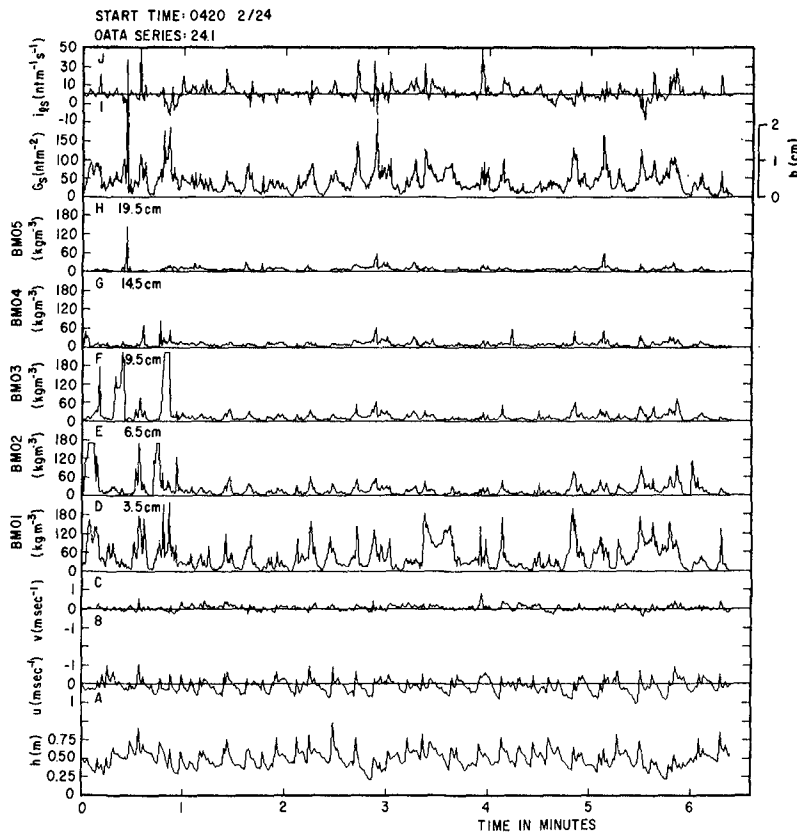


Fig. 6. A 7-min time series during data series 24.1.

are (A) water depth  $h$ , (B) on-offshore velocity component  $u$ , (C) longshore velocity component  $v$ , (D-H) suspended sediment mass concentration at five levels above the seabed, (I) total immersed weight suspended sediment load  $G_s$  and depth of erosion required to supply the suspended load  $b$ , (J) immersed weight suspended sediment longshore transport per unit width of seabed  $i_{ls}$ . The values of ( $G_s$ ), ( $b$ ), and ( $i_{ls}$ ) were computed every 1/2 s using the following equations:

$$G_s = \frac{\rho_s - \rho}{\rho_s} g \int_0^h C dz \quad (1)$$

$$b = \frac{\int_0^h C dz}{\rho_s C_b} \quad (2)$$

$$i_{ls} = G_s v \quad (3)$$

where  $\rho_s$  and  $\rho$  are sediment and fluid density;  $g$  is acceleration of gravity,  $C$  is suspended sediment mass concentration,  $h$  is total depth, and  $C_b$  is the volume concentration of the seabed (0.6), and  $v$  is longshore component of velocity.

The second category of analysis involved the computations of mean values of various sediment parameters. The averaging period for these computations was taken as 2048 s or approximately 34 min. This period is thought to be sufficiently long to give stable averages and yet short enough to minimize tidal variations during the averaging period. The mean suspended sediment concentration at each level above the bed ( $C$ ) and the mean immersed weight suspended sediment load ( $G_s$ ) were determined by averaging the values of  $C$  and  $G_s$  over 2048 s.

The third category of analysis included computations of immersed weight suspended sediment transport rate from the field measurements and the prediction of the total longshore transport rate using the methods of (16,17). The local immersed weight longshore transport rate of suspended sediment ( $\bar{i}_{ls}$ ) occurring at each sensor array was computed as shown in equation (4) and the total longshore transport rate of suspended sediment ( $I_{ls}$ ) was determined by summation of the individual measurements of  $\bar{i}_{ls}$  made across the surf zone (eq. 5). Equations 6 and 7 outline the computational methods for predicting the total longshore transport rate of sediment as developed by (16,17):

$$\bar{i}_{ls} = \overline{G_s v} \quad (4)$$

$$I_{ls} = \sum \bar{i}_{ls} \Delta X \quad (5)$$

$$I_l = K P_l \quad \text{where } K = 0.77 \text{ and } P_l = (E C_n)_b \sin \alpha_b \cos \alpha_b \quad (6)$$

$$I_l = K' (E C_n)_b \frac{\bar{v}_l}{u_m} \quad \text{where } K' = 0.28 \quad (7)$$

where  $X$  is distance from shoreline,  $(EC_n)_b$  is the wave-energy flux at the breaker,  $\alpha_b$  is the breaker angle,  $v_L$  is the longshore current velocity at the mid-surf position,  $U_m$  is the maximum horizontal orbital velocity evaluated at the breaker zone,  $K$  and  $K'$  are dimensionless coefficients determined empirically, and other terms are as defined above.

Because of the small number of sensor arrays deployed, measurements of  $I_{ls}$  made at different stages of the tide (and hence for different values of  $X/X_b$ ) during a data series were combined to increase data coverage across the surf zone.

#### Waves and currents

Various characteristics of the waves at breaking are required to calculate the littoral transport rate (eqs. 6 and 7). These include breaker height, breaker depth, breaking angle, and bottom oscillatory velocity. As all the variables were not measured throughout the experiment (e.g., angle of breaking), predictions of breaker characteristics for each data series were made using offshore pressure data. Waves measured at the offshore wave array (see Fig. 1) were subjected to computer analysis that included considerations of refraction and breaking. Where possible the predicted breaking characteristics were compared to the observed breakers to test the methods; however, the predicted breaker characteristics were used for calculations of littoral transport. The detailed procedure for this analysis and a data tabulation is given in (24). The measured longshore velocity used in eq. 7 was estimated by plotting values of  $\bar{v}$  obtained from the current meters placed across the surf zone and interpolating between points to  $X/X_b = 0.5$ . The values of  $P_1$  and  $(EC_n)_b \bar{v}_1/u_m$  (eqs. 6 and 7) were computed using rms rather than significant wave conditions to be consistent with other studies.

## RESULTS AND DISCUSSION

#### Suspended sediment

Some general observations of suspended sediment characteristics from data series 24.1 are summarized as follows:

- 1) The suspended sediment concentration near the seabed ( $z = 3.5$  cm) varied over a wide range and reached  $180 \text{ kg m}^{-3}$  during individual suspension events (Fig. 6D). The depth of erosion ( $b$ ) required to supply the measured suspended load is approximately 1-2 cm and is comparable to the mixing depth evaluated in various sand tracer studies (9,18).
- 2) The concentration decreased systematically away from the seabed (Fig. 6D-H).
- 3) Individual suspension events were in phase with bores propagating across the surf zone. Where the offshore directed flow prior to an incoming bore attained significant magnitude (i.e., the threshold of grain motion was exceeded), a sediment suspension event was initiated and then reinforced by the passage of a bore propagating shoreward.

4) The frequency and duration of sediment suspension events were strongly correlated with incident wave conditions. Low frequency oscillations of onshore/offshore velocity and water level were observed in many data records. Large temporal variations in the magnitude of suspension events also occurred; they appear to be of greatest magnitude in relation to major offshore flows of water corresponding to troughs in the low frequency signals.

Four representative suspended sediment profiles from data series 24.1 are shown in Figure 7. Two are from the breaker region ( $X/X_b = 0.84, 0.96$ ) and two are from the mid-surf zone ( $X/X_b = 0.49, 0.60$ ). The position of the lowest sensor in these profiles was 3.5 cm above the seabed which is over 150 grain diameters above the boundary ( $M_d = 0.23$  mm); thus any particles measured by the sensors are considered as suspended load (6,23). The dominance of suspended load transport at  $z = 3.5$  cm is also suggested by the maximum measured volume concentration of solids being 0.07 which is below the minimum volume concentration (0.08 or 0.09) considered necessary to produce a bedload transport layer supported by intergranular collisions (1,2,8). A generalized suspended sediment profile (11,12), collected shoreward of the breaking point, which was considered to be representative of suspended sediment profiles

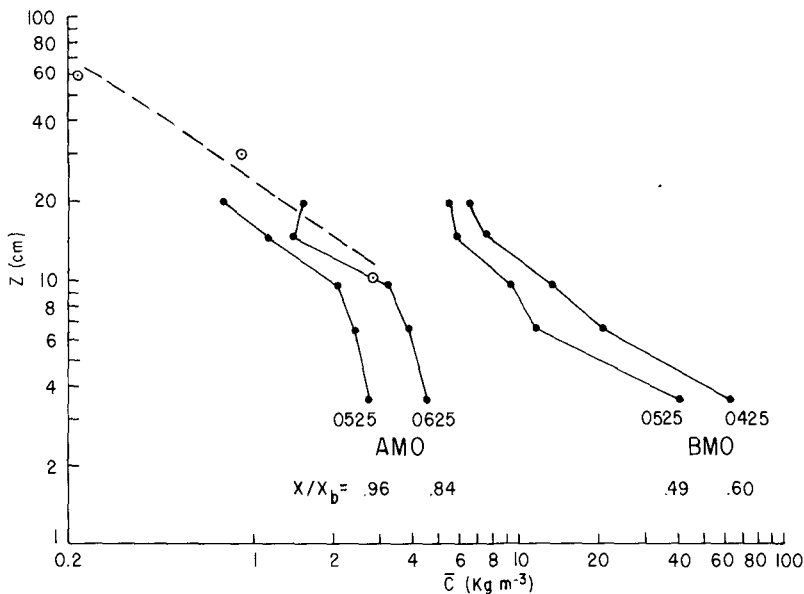


Fig. 7. Vertical profiles of mean values of suspended sediment from two sensor arrays during data series 24.1. Time of day indicates beginning of each averaging period and  $X/X_b$  indicates relative position across the surf zone where  $X_b$  equals breaking point. Open circles and dashed line are explained in the text.

associated with plunging breakers, is included (Fig. 7). The profiles plotted from data series 24.1 generally are similar to previous results (11,12). The mean concentration measured at  $z = 10$  cm for data series 24.1 ranges from approximately  $2\text{--}12 \text{ kg m}^{-3}$ , compared to  $3 \text{ kg m}^{-3}$  reported by (11,12), and the concentration increases logarithmically toward the seabed.

#### Sediment transport

The longshore transport rate of suspended sediment ( $I_{xs}$ ) was determined for each of the six data series (Fig. 8). Values of  $I_{xs}$  were plotted according to their relative position within the surf zone ( $X/X_b$ ), and the area encompassed by the points is proportional to  $I_{xs}$ .

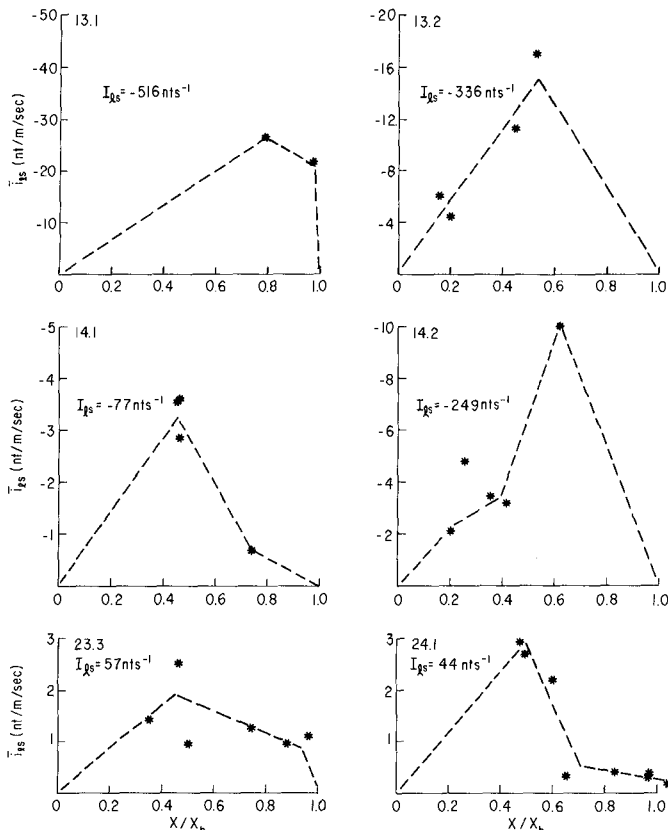


Fig. 8. Cross-shore distribution of  $I_{xs}$ . The total longshore transport rate ( $I_{xs}$  from eq. 5) is noted for each curve.

The curves have been extended to zero at the positions of  $X/X_b = 0$  and 1.0. Thus, any swash zone transport or transport beyond the breaker point was not considered. The shapes of the curves, although irregular, follow a general pattern, with maximum longshore transport approximately in the mid-surf position. The data points tend to be grouped on either the shoreward or the seaward side of  $X/X_b = 0.5$ , and no single data series spanned the width of the surf zone. Nevertheless, visual inspection of the six data series appears to justify the way in which the curves are extrapolated to zero. This general distribution of  $I_{ls}$  suggested by previous field measurements (3,11), laboratory measurements (19), and theoretical predictions (14). The area under each curve multiplied by the width of the surf zone represents the measured value of  $I_{ls}$  (Fig. 8 and Table 1).

Table 1. Longshore transport calculations.

Data Series	Average $P_l$ (nt/s)	Average $(ECn)_b v_l/u_m$ (nt/s)	Width $X_b$ (m)	Beach slope $\beta$	Measured $I_{ls}$ (nt/s)	K	K'
13.1	-203	-1470	34	0.041	-516	2.54	0.35
13.2	-374	-2360	48	0.041	-336	0.90	0.14
14.1	-229	-462	55	0.037	-77	0.34	0.17
14.2	-278	-618	60	0.037	-249	0.89	0.40
23.3	19	207	55	0.022	57	3.00	0.28
24.1	17	75	35	0.021	44	2.59	0.59
		Average	0.033			1.71	0.32

It is also of interest to know how the longshore transport rate of suspended sediment compares with the estimated total littoral transport rate. Assuming that equations 6 and 7 predict the total longshore transport rate ( $I_l$ ), as discussed by (16), the ratio of  $I_{ls}$  to  $I_l$  represents the contribution of suspended sediment to the total. In Figures 9A and B the values of  $I_{ls}$  from this study (solid circles) have been superimposed on a plot from (16).

In Figure 9A the data from this study tend to fall above the predictive line while the agreement in Figure 9B is excellent. The average value of K is 1.71, approximately twice the value determined from previous studies (eq. 6,  $K = 0.77$ ), whereas that of K' is 0.32 which is within 14% of the value determined previously (eq. 7,  $K' = 0.28$ ).

According to (16), equation 7 (Fig. 9B) is the more fundamental of the two sand transport relationships and should be applicable regardless of the origin of the longshore current ( $\bar{v}_l$ ), e.g., tide or wind generated, and currents of the cell circulation, or of oblique wave approach. It was also pointed out by (16) that it is usually easier to measure the longshore current than the breaker angle needed in the evaluation of  $P_l$  in equation 6. Further, it was demonstrated (18) that equation 7 is applicable where the longshore current was the net result of two opposing currents. The close agreement between the results of this study and previous studies (Fig. 9B) suggests that all of the longshore transport at Leadbetter Beach can be accounted for by suspended

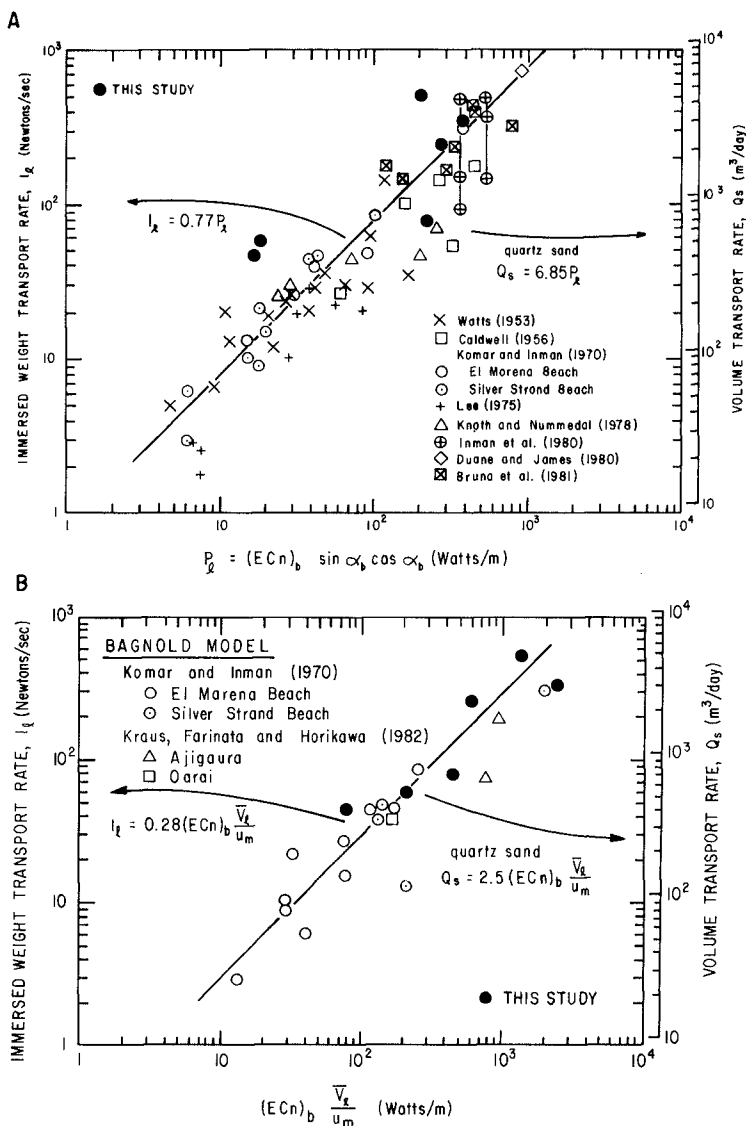


Fig. 9. Measurements of sand transport rates on beaches compared with wave conditions expressed as  $P_g$  of eq. 6 (A); eq. 7 (B) (16). Data from this study are superimposed on each curve.

sediment transport and that equation 7 adequately predicts the total immersed weight longshore transport rate of suspended sediment in the surf zone.

The ratio of  $I_{ls}$  to  $I_l$  is significantly higher than has been generally measured or estimated by other investigators (Table 2).

Table 2. Ratio of suspended sediment to total longshore sediment transport rate.

Study	Lowest Measurement (cm)	$\frac{I_{ls}}{I_s}$
Komar (1978) (15)	7.6-10	0.07-0.26
Inman et al. (1981) (9)	10	0.15-0.20
Kana and Ward (1981) (13)	5	1.0
	post-storm	0.30
Downing (1983) (3)	3.5	0.47
This study	3.5	1.0

Although it would be expected that physical processes in the surf zone would have a major influence on sediment suspensions and hence might account for the differences observed above, there are also major differences in sampling techniques that play an important role.

The relative quantities of suspension transport versus bedload transport was analyzed by (15) who developed an equation to estimate the ratio  $I_{susp}/I_{total}$  ( $= I_{ls}/I_l$ ). The important parameters in this equation are the mean volume concentration ( $\bar{c}$ ), beach slope ( $\tan \beta$ ), and ratio of breaker height to breaker depth ( $\gamma$ ). The analysis included pump data (5,25) and diver collected data (10). Sediment samples were collected no closer than 7.6 cm from the seabed and the results suggest that the value of  $I_{ls}/I_l$  is  $\leq 0.26$ .

In another study (9) using diver-operated samplers, suspended sediment samples were not collected within 10 cm of the seabed; the ratio of  $I_{ls}/I_l$  was 0.15-0.20. Bulk water samplers (13) were mounted from a pier with the lowest 5 cm above the seabed. During storm conditions the ratio of  $I_{ls}$  to  $I_l$  was high, similar to our results. During post-storm conditions, however, the value of  $I_{ls}/I_l$  decreased to 0.30.

A study (3) using sensors and methods similar to the present study obtained a much lower  $I_{ls}/I_l$  ratio (0.47). Except for the experimental site being a wide dissipative beach rather than a narrow, reflective beach, the two studies were similar; the difference in  $I_{ls}/I_l$  is quite possibly related to dynamic processes.

For the present study the mean values of  $c$  for all data (average of  $G_s$  converted to volume concentration) is  $1.46 \times 10^{-3}$ ,  $\tan \beta = 0.033$ , and  $\gamma = 0.53$ . Using these values in the equation of (15) gives an estimate of  $I_{ls}/I_l = 0.92$  which is in agreement with the results shown in Figure

9B. This further suggests that our observations are consistent with previous analyses (15) and that  $I_{ls}/I_l$  is predictable on the basis of mean volume concentration, beach slope, and the breaker height to breaker depth ratio.

#### CONCLUSIONS

1. Sediment transport in the nearshore zone occurs as individual suspension events associated with bores propagating landward. Sediment concentrations as high as  $180 \text{ kg m}^{-3}$  are measured at 3.5 cm off the seabed under passing bores and may be greater than  $50 \text{ kg m}^{-3}$  at 55 cm elevation. Individual suspension events occur abruptly and may last only seconds. Temporal variations of the magnitude of suspension events are observed in most data records. These variations in magnitude appear to be related to the bore amplitude and low frequency oscillations of the velocity component within the surf zone.

2. Mean concentration profiles show an approximately logarithmic decrease away from the bed.

3. Maximum erosion depths required to supply each suspension event are approximately 1-2 cm, comparable to the mixing depth evaluated in various sand tracer studies.

4. The longshore transport rate of suspended sediment is maximum within the mid-surf region and decreases towards both the breaking point and the shore. Suspended sediment transport appears to be high in the swash-backwash region of the shore; however, detailed data analysis has not been completed.

5. The total immersed weight longshore transport rate of suspended sediment accounts for all of the total longshore transport rate as predicted by the equations developed by (16,17). The suspended sediment transport rate as measured during the experiments at Leadbetter Beach can be predicted by equation 7.

#### ACKNOWLEDGEMENTS

We would like to thank S. Woods and R. Johnson for their expert advice and fine craftsmanship in fabricating the instrumentation used for this study. H. Smith provided energetic assistance in gathering the field data and B. Jaffe assisted in the early stage of data analysis. This research was supported in part by a National Sea Grant (NOAA) contract #SGNOAA NA81 KA-D-0030 and Office of Naval Research Contract N00014-84-C-0111.

## REFERENCES

1. Bagnold, R.A.: 1963. "Mechanics of Marine Sedimentation." In Hill, M.N. (ed.), *The Sea* 3: 507-528. Wiley-Interscience, New York, NY.
2. Bailard, J.A. and D.L. Inman: 1979. "A Reexamination of Bagnold's Granular-Fluid Model and Bedload Transport Equation." *J. geophys. Res.* 84: 7827-7833.
3. Downing, J.P., Jr.: 1983. "Field Studies of Suspended Sand Transport, Twin Harbors Beach, Washington." Ph.D. Dissertation, University of Washington, Seattle, Washington.
4. Downing, J.P., R.W. Sternberg, and C.R.B. Lister: 1981. "New Instrumentation for the Investigation of Sediment Suspension Processes in the Shallow Marine Environment." In Nittrouer, C.A. (ed.), *Sedimentary Dynamics of Continental Shelves*: 19-34. Mar. Geol. 42 (Special Issue).
5. Fairchild, J.C.: 1973. "Longshore Transport of Suspended Sediment." Proc. 13th Coastal Engineering Conference: 1069-1088.
6. Francis, J.R.D.: 1973. "Experiments on the Motion of Solitary Grains Along the Bed of a Water-Stream." Proc. R. Soc. Lond. A. 332: 443-471.
7. Gable, C.G. (ed.): 1981. "Report on Data from the Nearshore Sediment Transport Study Experiment at Leadbetter Beach, Santa Barbara, California, January-February, 1980." 314 p.
8. Inman, D.L.: 1963. "Sediments: Physical Properties and Mechanics of Sedimentation." In Shepard, F.P., *Submarine Geology*: 101-151. 2nd Ed., Harper & Row Publishers, Inc., New York, New York.
9. Inman, D.L., J.A. Zampol, T.E. White, D.M. Hanes, B.W. Waldorf, and K.A. Kastens: 1981. "Field Measurements of Sand Motion in the Surf Zone." Proc. 17th Coastal Engineering Conference: 1215-1234.
10. Kana, T.W.: 1976. "A New Apparatus for Collecting Simultaneous Water Samples in the Surf Zone." *J. sedim. Petrology* 46: 1031-1034.
11. Kana, T.W.: 1979a. "Surf Zone Measurements of Suspended Sediment." Proc. 16th Coastal Engineering Conference: 1725-1743.
12. Kana, T.W.: 1979b. "Suspended Sediment in Breaking Waves." Tech. Rep. No. 8-CRD, Coastal Research Division, Department of Geology, University of South Carolina, Columbia, South Carolina.
13. Kana, T.W. and L.G. Ward: 1981. "Nearshore Suspended Sediment Load During Storm and Post-Storm Conditions." Proc. 17th Coastal Engineering Conference 2: 1158-1174.

14. Komar, P.D.: 1977. "Beach Sand Transport: Distribution and Total Drift." *J. Wat Way Port Coast. Ocean Div. Am. Soc. civ. Engrs* **103**(WW2): 225-239.
15. Komar, P.D.: 1978. "Relative Quantities of Suspension Versus Bed-Load Transport on Beaches." *J. sedim. Petrology* **48**: 921-932.
16. Komar, P.D.: 1983. "Nearshore Currents and Sand Transport on Beaches." In Johns, B. (ed.), *Physical Oceanography of Coastal and Shelf Seas*: 67-109. Elsevier Science Publishers B.V., Amsterdam, Netherlands.
17. Komar, P.D. and D.L. Inman: 1970. "Longshore Sand Transport on Beaches." *J. geophys. Res.* **75**: 5914-5927.
18. Kraus, N.C., R.S. Farinato, and K. Horikawa: 1981. "Field Experiments on Longshore Sand Transport in the Surf Zone." *Coast. Engng Japan* **24**: 171-194.
19. Sawaragi, T. and I. Deguchi: 1979. "Distribution of Sand Transport Rate Across a Surf Zone. *Proc. 16th Coastal Engineering Conference*: 1596-1613.
20. Seymour, R.J. (ed.): In press. "Nearshore Sediment Transport Study." Plenum Press, New York.
21. Seymour, R.J. and D.B. Duane: 1979. "The Nearshore Sediment Transport Study." *Proc. 16th Coastal Engineering Conference*: 1555-1562.
22. Seymour, R.J. and C.G. Gables: 1980. "Nearshore Sediment Transport Study experiments." *Proc. 17th International Conference on Coastal Engineering*: 1402-1415.
23. Smith, J.D. and T.S. Hopkins: 1972. "Sediment Transport on the Continental Shelf Off of Washington and Oregon in Light of Recent Current Measurements." In Swift, D.J.P., D.B. Duane, and O.H. Pilkey (eds.), *Shelf Sediment Transport: Process and Patterns*: 143-180. Dowden, Hutchinson and Ross, Inc., Stroudsburg, Pennsylvania.
24. Sternberg, R.W.: In press. Suspended Sediment Measurements. A. Continuous Measurements. In Seymour, R.J. (ed.), *Nearshore Sediment Transport Study*. Plenum Press, New York.
25. Watts, G.M.: 1954. "Field Investigation of Suspended Sediment in the Surf Zone." *Proc. 4th Conference on Coastal Engineering*: 181-199.